DEVELOPMENT OF FINITE ELEMENT MODEL FOR CHILD PEDESTRIAN PROTECTION

Masayoshi Okamoto
Yukou Takahashi
Honda R&D Co., Ltd.
Fumie Mori
PSG Co., Ltd.
Masahito Hitosugi
Dokkyo University School of Medicine
JAPAN
Jane Madeley
Johan Ivarsson
Jeff R. Crandall
University of Virginia
United States of America
Paper Number 151

ABSTRACT

In recent years, pedestrian protection has been increasing its importance in the field of vehicle crash safety. Under such circumstances, the European Enhanced Vehicle-safety Committee (EEVC) has proposed a test procedure for evaluating injuries to pedestrians in car-pedestrian accidents. This test procedure covers potential injuries to the adult head, pelvis, and lower limb, while only the head region is covered for children.

A number of child finite element (FE) models have been published for understanding injury mechanisms in child pedestrians. However, most of these models have been constructed by geometrically scaling an adult model. These scaled models do not take into account the specific anatomical structures in children, which do not allow these models to reproduce injuries exclusively observed in child pedestrians. In addition, the lack of sufficient in-depth accident data for child pedestrians leads to a need for a child FE model that accurately represents these specific structures, and is capable of reproducing injury mechanisms in child pedestrians.

This paper describes a preliminary FE model for a child pedestrian constructed using the MRI scans from a 6-year-old child. In the future, this model will be used for injury mechanism analysis and injury criteria development for child pedestrians.

INTRODUCTION

In addition to occupant protection in car crashes, pedestrian protection has become an important issue in vehicle crash safety. In pedestrian protection research, techniques such as component tests, full-scale tests, and computer simulation are generally employed. Among these methods, a test procedure proposed by the EEVC has been most commonly used in the development of technologies for pedestrian protection, and has been considered as one of the potential bases for the future regulations. However, with the exception of the child headform, this test procedure has been designed for evaluating injuries to adult pedestrians. This does not allow for injuries to other child body regions to be addressed.

An alternative means for assessing injuries to child pedestrians is to develop an FE child model. This approach essentially requires data for the material properties of tissues and impact responses of children. Due to ethical issues, however, experimental studies for obtaining these mechanical properties are limited to some old studies. For these reasons, past studies for developing a child FE model have used estimated material properties by applying scaling techniques to adult properties. In addition, the geometry of these models has been obtained by scaling an adult model.

The goal of this study was to develop an FE child model in standing position that reflects specific anatomical structures in children. The geometry of the model was based on the MRI scans from a child volunteer. The project is still ongoing, and the FE models for the lower limb skeletal and major connective tissues as well as the surface geometry of the whole body are currently available. A methodology for developing a child FE model from MRI scans will be presented in this paper. The lower limb model developed in this study will also be illustrated in comparison with the actual MRI scans.

ACCIDENT DATA ANALYSIS

According to accident statistics [1], pedestrian fatalities account for 37 % in South Korea, 28 % in Japan, 25 % in the UK of all fatalities due to traffic accidents. Even the Netherlands with the lowest percentage of pedestrian fatalities has the contribution from pedestrians of as much as 10 % (Figure 1).

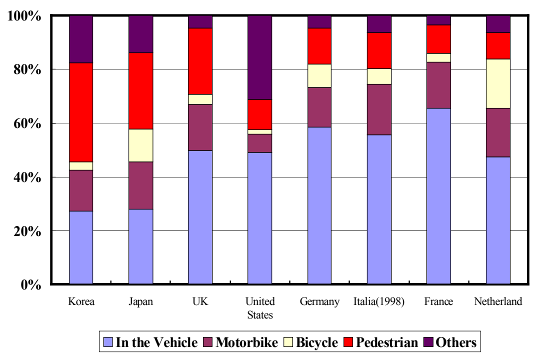

Figure 1. Distribution of fatalities in traffic accidents by accident type.

Figure 2 shows the distribution of fatalities by accident type and age in Japan. In the age bands of 12 years old and younger, and 70 years old and older, pedestrian accidents account for approximately 50 % of all fatalities in traffic accidents.

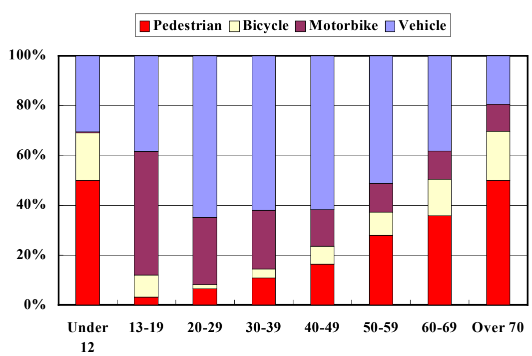

Figure 2. Distribution of fatalities in traffic accidents by accident type and age in Japan.

The distribution of pedestrian fatalities and injuries in Japan by age for year 2001 is presented in Figure 3. For the age bands younger than 50 years old, the number of fatalities per year was roughly 100, while the number of fatalities increased for the older age bands. For injuries, the most frequent age band was 12 years old and younger with approximately 20,000 injuries, followed by the older populations.

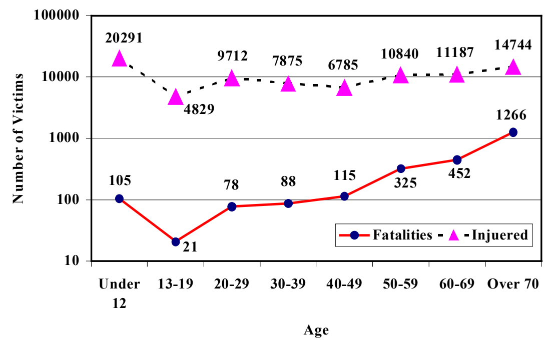

Figure 3. Distribution of pedestrian fatalities and injuries by age in Japan (2001).

These results suggest that the younger generation (12 years old and younger) and older generation (50 years old and older) are the most important for mitigating pedestrian fatalities and injuries. In these generations, the older generation should have the anthropometry of adults, suggesting that the currently proposed test procedures for adults such as the EEVC test procedure can potentially cover this generation in terms of the anthropometry. Since the current test procedure covers only the head region of children, the remaining issue would be to determine the direction of countermeasures for mitigating injuries to other body regions.

Figure 4 illustrates the distribution of severe injuries to child pedestrians, 12 years old and younger, in Japan for year 2001. The head and lower limb injuries account for 18 % and 60 %, respectively, of all severe injuries, while other data sources show that the head injuries account for approximately 70 % of all fatalities. Injuries to other body regions (upper limb, thorax, abdomen) account for 22 % in total. This suggests that the protection of the child lower limb is one of the most important issues for mitigating severe injuries to pedestrians.

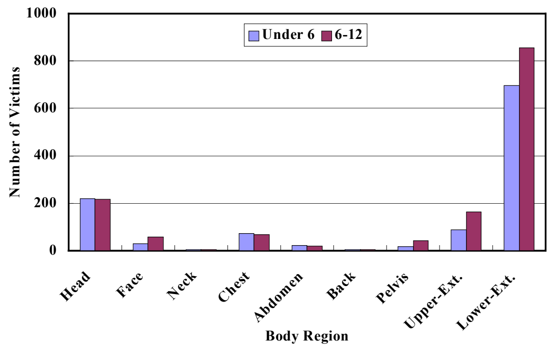

Figure 4. Distribution of severe injuries to child pedestrians (12 years old and younger) in Japan (2001).

DEVELOPMENT OF CHILD FE MODEL

Background

One of the biggest issues in the development of an FE model for a child pedestrian is that the data for precise geometry and material properties are not available. In previous studies for child model development, the geometry and material properties were estimated by applying a scaling technique to the data for adults. However, a child is still growing, resulting in some specific features in its anatomical structure.

One of the most significant anatomical features is related to development of the bony structure. The child skeleton is first laid down as a cartilage template in the embryo. Over time this is gradually replaced with bone in a process known as ossification which occurs at the same time as skeletal growth. Two kinds of ossification are recognized – the membranous ossification, and the endochondral ossification. The membranous ossification occurs in the flat bones, e.g. cranial and facial bones, while the endochondral ossification occurs in the tubular bones during development and growth. In long bones, the length of the bone increases by the process called interstitial growth. In the cartilage template this process may occur throughout the structure, but following the onset of ossification longitudinal growth occurs only at the growth plate which remains cartilaginous until the final length of the bone has been reached. The growth plate ossifies slowly throughout childhood and the cartilage finally disappears between the ages of 18 and 25 years. At this point the bone loses its potential for longitudinal growth. Growth in diameter is by a process called appositional growth. In the cartilage template, cartilage is laid down circumferentially by the cells of the perichondrium, and this process continues in the bone as layers of bone are laid down by the inner cells of the periosteum. These processes of growth result in specific anatomical structures for child long bones in the epiphyses, growth plates, metaphyses, and diaphyses (Figure 5).

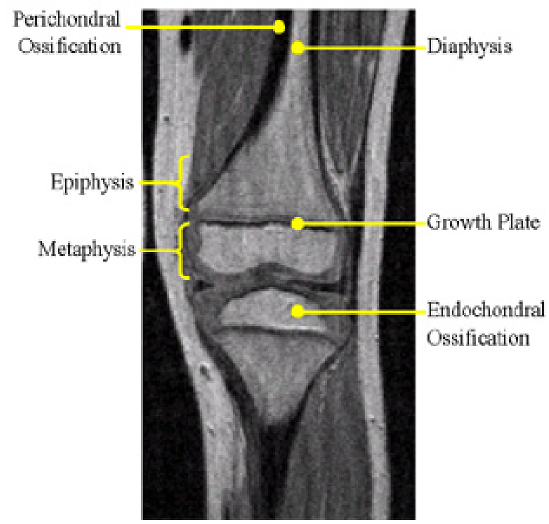

Figure 5. Anatomical regions of the child long bones with specific features.

In terms of the material properties of bones in children, child bones are generally characterized by the following features as compared with adult bones:

1. Child bones are more flexible than those of an adult due to low bone mineral content [3][4]
2. Child bones are more porous than those of an adult; this may result in terminating the fracture propagation in bones [5]
3. Cartilaginous growth plates, exclusively seen in children, are vulnerable to shear force [6][7]

These features are believed to be responsible for some specific fracture patterns such as plastic bowing, greenstick, and buckling (Figure 6) [8]. Some fracture patterns at the growth plate are also reported (Figure 7) [9].

These features exclusively observed in children suggest that the models for child skeleton based solely on the scaling technique applied to the geometry of adult bones have limitations in reproducing injuries to children.

On the other hand, based on the recent advancement in digital image processing technologies, three-dimensional anatomical models of a patient have been actively generated from the CT or MRI scans in medical science. In this study, MRI scans of an actual child volunteer were taken. These scans have been used to generate an FE child model that takes into account specific anatomical features in children.

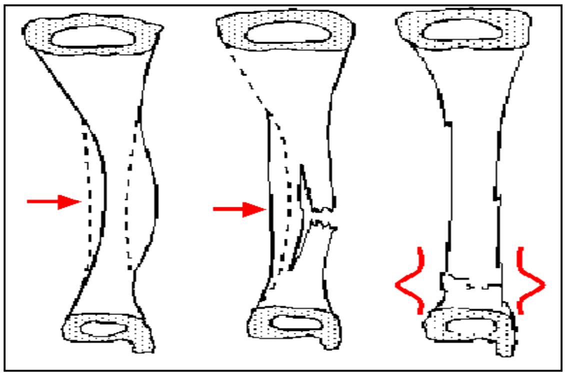

Figure 6. Specific fracture patterns in child tibia.

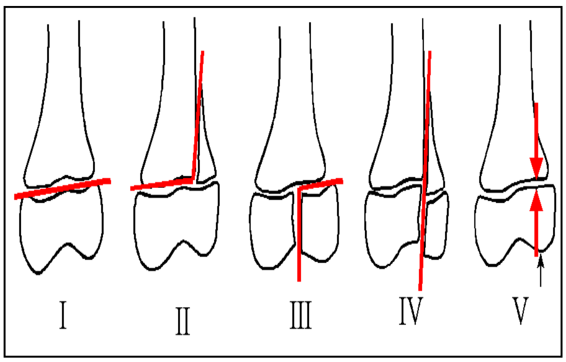

Figure 7. Classification of growth plate injury in children.

Ethical Standard

The World Medical Association has developed the Declaration of Helsinki as a statement of ethical principles to provide guidance to physicians and other participants in medical research involving human subjects [10]. In this declaration, it is described that the design and performance of each experimental procedure involving human subjects should be clearly formulated in an experimental protocol. This protocol should be submitted for consideration, comment, guidance, and where appropriate, approval to a specially appointed ethical review committee, which must be independent of the investigator, the sponsor or any other kind of undue influence. This independent committee should be in conformity with the laws and regulations of the country in which the research experiment is performed. In addition, it is described that when a subject deemed legally incompetent, such as a minor child, is able to give assent to decisions about participation in research, the investigator must obtain that assent in addition to the consent of the legally authorized representative. This study followed the procedure described in this declaration. Prior to performing the scan, the contents of the research were explained to both the subject and its custodian, and consent was obtained.

In this research, the ethics regulation described above was followed, and the MRI experiment was approved by the Ethics Committee at the Advanced Telecommunications Research Institute International (ATR). The scan was made at the Brain Activity Imaging Center at ATR. Considering the age of the subject (6 years old), it was required from the Ethics Committee that the custodian should have accompanied with the subject throughout the experiment, and the experiment should have been immediately terminated upon request from the subject. In addition, a medical doctor joined the experiment for periodical medical checks during the experiment.

Methodology

Image Scanning

The following four ways are generally available for scanning a human body:

1. Radiography
2. Ultrasound Imaging
3. X-ray Computed Tomography (X-rays CT)
4. Magnetic Resonance Imaging (MRI)

X-rays scanning is capable of obtaining images of anatomical structures with very high resolution. However, X-ray contamination is problematic with the health condition of the subject. Although this method is very effective for matured bony structures, it is difficult to obtain accurate geometry for soft tissues such as the articular cartilage and immature growth plate in children due to their X-ray transparency [11]. The scanning with ultrasonic waves only provides low resolution and quality of images. Although the resolution of images is lower than that from X-rays, this study employed MRI scanning since clear images for not only hard tissues, but also soft tissues, can be obtained. A past study succeeded in reconstructing the detailed anatomical structure of a human body using MRI scans.

Apparatus

The scans were performed using the MRI system at the Brain Activity Imaging Center in ATR. The system was operated by the technicians at this center. The specification of the system used in this study is listed below:

MRI scanner : Shimazu-Marconi MAGNEX ECLIPS 1.5T Power Drive 250 (Figure 8)
Magnet subsystem
Homogeneity : < 1 ppm / 50 cm DVS
Gradient subsystem
Design : direct drive / non-resonant
Scanning capability : 3-axes, full oblique
Peak strength : 27 mT/m
Ramp Rate : 72 mT/m/ms
Radio frequency subsystem
Output power : 25 kW
Image processing
CPU : DEC Alpha XP1000, 64bit/500MHz
Image reconstruction : 0.02 s/slice or 50 slices/s with 256 x 256

Figure 8. MRI scanner used in this study.

Anthropometry

Average height and weight as a function of age and gender were compared among countries all over the world. [12] The results suggested that there was no significant difference between countries and gender up to 12 years old. Figures 9 and 10 show the distribution of the world average height and weight, respectively, as a function of age and gender. The height and weight of the 6-year-old child volunteer, whose MRI scans were taken in this study, were 110.9 cm and 19.5 kg, respectively. The world average height and weight of a 6-year-old child were 114.6 cm (standard deviation: 3.7 cm) and 20.4 kg (standard deviation: 1.76 kg), respectively. Therefore, the height and weight of the child volunteer were within one standard deviation of the world average, suggesting that the anthropometry of the volunteer can be regarded as representative of the average 6-year-old child worldwide.

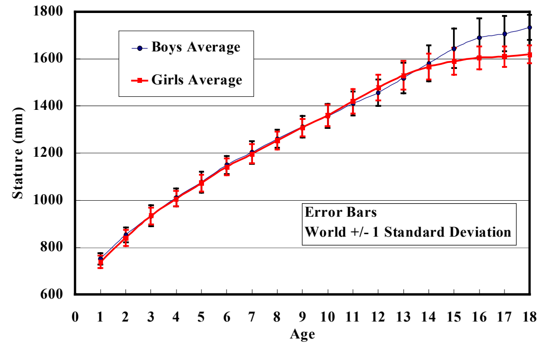

Figure 9. Distribution of world average stature as a function of age and gender.

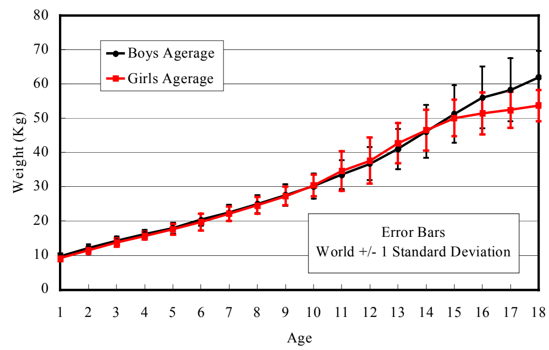

Figure 10. Distribution of world average weight as a function of age and gender.

Scanning

Considering that the volunteer is a child, and thus prolonged scanning was deemed unfavorable, it was decided that the duration time of each scan be limited to 10 minutes maximum. The entire body was divided into 11 body regions, and one region was scanned at a time.

The resolution of the images (Voxel Size) can be determined as a function of the range of covered area (Field Of View: FOV), the size of the images (Matrix), and the pitch of image acquisition. The maximum Matrix of the MRI system employed in this study was 512*512, however, the Matrix of 256*256 was used in order to reduce the duration time of each scan. The pitch between slices was determined between 1.5 mm and 4 mm, depending on the body regions, so that the duration time of the scanning can be minimal. The images were collected with the Voxel Size between 0.5*0.5*1.5 and 1.17*1.17*4 (x*y*slice pitch). The scanning directions were selected from transverse, sagittal, and coronal directions, depending on the body regions, so that the anatomical structures to be reconstructed can be best described in the scans (Table 1).

Region	Orientation	Slices (Pieces)	FOV (mm)	Matrix Pixel	Thickness (mm)	Voxel Size
Head	Transverse	65	256	256x256	4	1.0x1.0x4.0
	Coronal	No Data				
	Sagittal	41	256	256x256	4	1.0x1.0x4.0
Neck	Transverse	65	256	256x256	4	1.0x1.0x4.0
	Coronal	No Data				
	Sagittal	62	256	256x256	1.5	1.0x1.0x1.5
Thorax	Transverse	43	256	256x256	5	1.0x1.0x5.0
	Coronal	74	256	256x256	2	1.0x1.0x2.0
	Sagittal	90	300	256x256	4	1.17x1.17x4.0
Shoulder	Transverse	No Data				
	Coronal	No Data				
	Sagittal	72	128	256x256	1.5	0.5x0.5x1.5
Upper Arm	Transverse	72	128	256x256	1.5	0.5x0.5x1.5
	Coronal	No Data				
	Sagittal	No Data				
Forearm	Transverse	59	128	256x256	4	0.5x0.5x4
	Coronal	No Data				
	Sagittal	No Data				
Abdomen	Transverse	72	128	256x256	4	0.5x0.5x4
	Coronal	74	256	256x256	2	1.0x1.0x2.0
	Sagittal	No Data				
Upper Leg	Transverse	84	256	256x256	4	1.0x1.0x4.0
	Coronal	No Data				
	Sagittal	65	256	256x256	2	1.0x1.0x2.0
Knee	Transverse	No Data				
	Coronal	44	192	256x256	1.5	0.75x0.75x1.5
	Sagittal	53	192	256x256	1.5	0.75x0.75x1.5
Lower Leg	Transverse	59	192	256x256	1.5	0.75x0.75x1.5
	Coronal	No Data				
	Sagittal	No Data				
Foot	Transverse	73	256	256x256	4	1.0x1.0x4.0
	Coronal	116	192	256x256	1.5	0.75x0.75x1.5
	Sagittal	47	192	256x256	1.5	0.75x0.75x1.5

Table 1.
Matrix of MRI scanning

__Process of 3D FE Modeling__

In order to utilize the MRI scans in three-dimensional FE modeling, the two-dimensional images obtained from MRI scans need to be converted to a three-dimensional structure. The following procedure was used to obtain three-dimensional FE meshes from the MRI scans.

1. The contour of the anatomical structure to be reconstructed was tracked for each slice image (Figure 11).

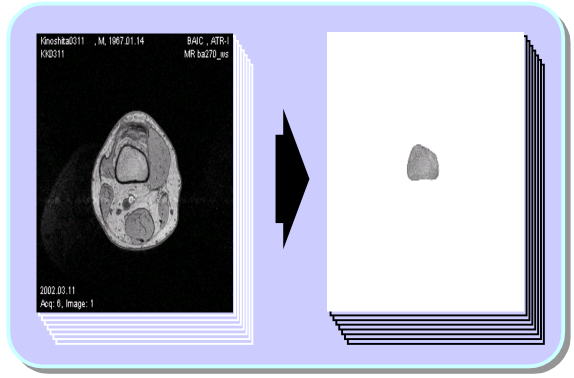

Figure 11. Edit the Classification region with PC.

2. A three-dimensional polygon model was obtained by interpolating the contours generated in step 1 in the scanning direction. In this study, the Forge^{TM} Ver. 1.5 (Studio PON) was used on a PC to create the polygon data (Figure 12).

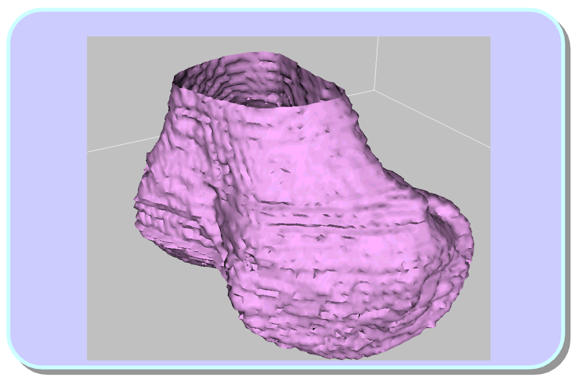

Figure 12. Transform the 2D data to 3D data.

3. Based on the three-dimensional polygon data, FE meshes were generated using shell and solid elements. (Figure 13)

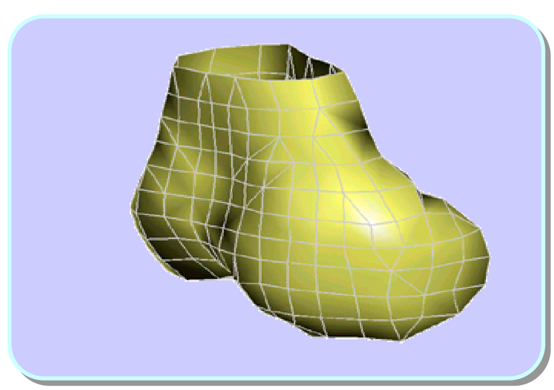

Figure 13. Make FE shell/Solid model.

Child FE Model

According to the currently available accident statistics, approximately 70 % of all fatalities in child pedestrians are due to head injuries. As a tool for evaluating head injuries to child pedestrians, the EEVC test procedure using a child headform is currently proposed, and is considered as one of the bases for the future regulation. On the other hand, more than twenty thousand children in Japan sustained severe injuries in car-pedestrian accidents each year, and the most frequently injured body region was the lower limb, accounting for approximately 60 % of all severe injuries to child pedestrians. The final goal of this study is to develop a full-body FE model for a child pedestrian. Based on this observation, however, it was decided to prioritize the development of the lower limb region. Since the currently proposed test procedure does not cover the lower limb of a child pedestrian, it was expected that the development of the child lower limb model at an early stage would facilitate mitigation of severe injuries to child pedestrians.

Since Honda R&D has been developing an FE lower limb model for an adult pedestrian [13] using PAM-CRASH™, the same program was used to develop an FE child model. The same modeling strategy as that of the adult lower limb model was applied to the child model. The soft tissues surrounding the bony structure (muscles and fatty tissues) were modeled using solid elements. On the surface of these soft tissues, the skin was modeled using shell elements in order to take into account its mechanical contribution to the knee joint response (Figure 14).

In order to accurately reproduce the mechanical response of each knee ligament due to the knee joint deformation, three of the four major knee ligaments (Anterior Cruciate Ligament; ACL, Posterior Cruciate Ligament; PCL, Lateral Collateral Ligament; LCL) were modeled using solid elements. The Medial Collateral Ligament (MCL) was modeled using shell elements considering its thinness. It was difficult to identify the exact geometry of some portions of ligaments. For these regions, FE meshes were generated by referring to anatomy books. The superior and inferior insertion sites of the ligaments were rigidly attached to the corresponding parts of bones. The models for the menisci obtained from the MRI scans

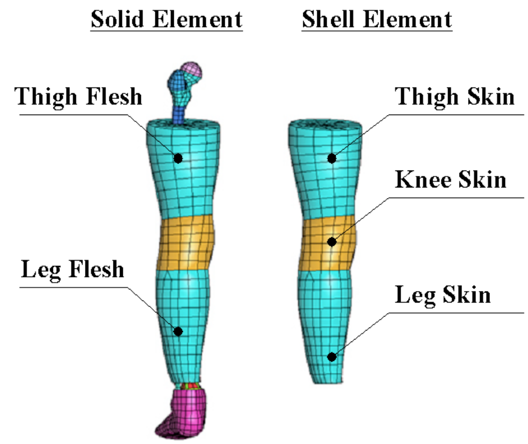

Figure 14. FE Models for lower limb flesh and skin.

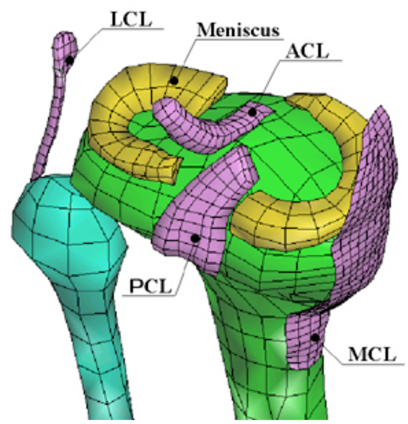

Figure 15. Models for major knee ligaments and menisci.

were placed on the tibial plateau in order to accurately simulate the knee joint stiffness in axial compression (Figure 15).

One of the biggest advantages of FE modeling from the MRI scans of an actual child is that the model is capable of accurately representing the anatomical features exclusively seen in children, including cartilaginous structures in the epiphyseal region of the child long bones. In the MRI scans of the child lower limb, these cartilaginous structures can be recognized in the femoral head, femoral condyles, tibial condyles, and growth plates. In order to simulate specific fracture patterns initiated at these cartilaginous structures in children, the model included the occification centers at the femoral head, femoral and tibial condyles, and ankle, the epiphyseal cartilage at the proximal and distal end of the femur and tibia, and the cartilaginous growth plates. These structures were modeled using solid elements

(Figures 16-18). For the pelvis and above, only the surface skin modeled using shell elements is available at this time (Figure 19). The bony structures as well as connective tissues in this region will be reconstructed in a future study.

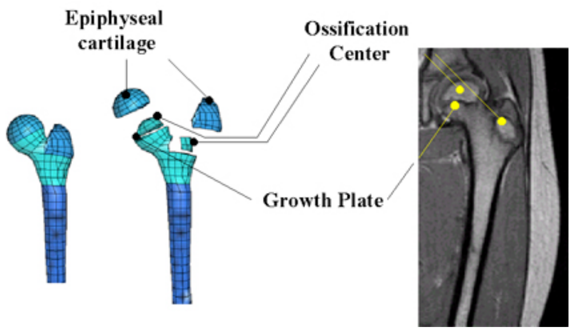

Figure 16. Child FE model for proximal femur.

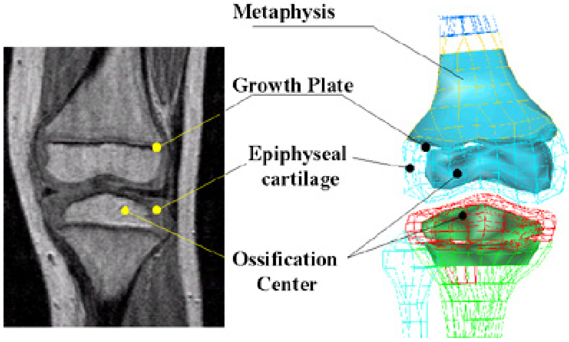

Figure 17. Child FE model for knee joint.

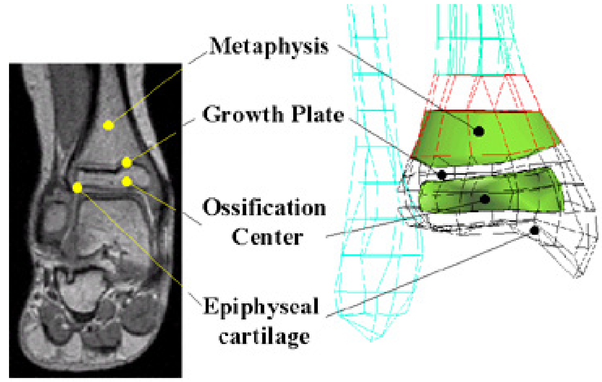

Figure 18. Child FE model for distal tibia/fibula.

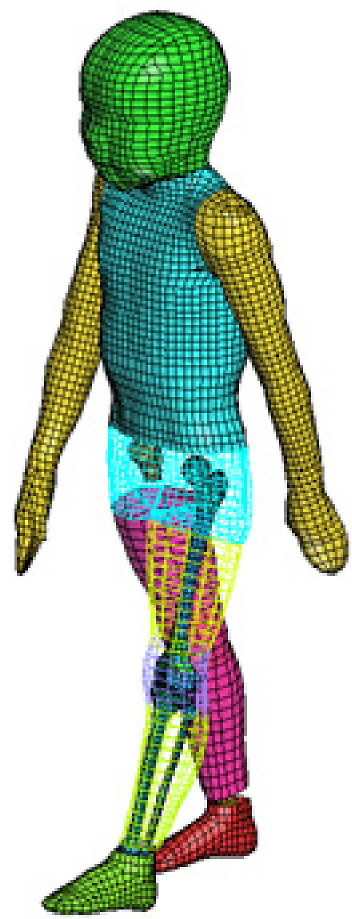

Figure 19. Child Whole Body FE model.

CONCLUSIONS

1. MRI scans of the whole body of a 6-year-old child were taken. Based on the MRI data obtained, a preliminary FE lower limb model for a child pedestrian was developed.
2. For reproducing specific fracture patterns in children, the geometry of the cartilaginous structures at the femoral head, knee, and ankle were precisely reconstructed from the MRI scans, and was included in the FE lower limb model.

FUTURE WORK

The currently ongoing study focuses on determining the material properties to be used as input into the FE model developed here. Once appropriate material properties are determined, the effect reflecting specific anatomical features in children has on reproducing fracture patterns exclusively observed in children will be investigated. The model will also be validated against results of in-depth accident data for car-child pedestrian impact. In addition, the finite element portion of the model will be expanded to the pelvis and above for skeletal and connective tissues.

ACKNOWLEDGEMENT

The authors would like to thank the child volunteer and his custodian for understanding the keystone of this research, and willingly cooperating with the scanning. They also would like to thank the staff at the Advanced Telecommunications Research Institute, Brain Activity Imaging Center, for providing an opportunity to use their MRI system, cooperating for obtaining approval from the Ethics Committee, and providing precious comments for minimizing the load to the child volunteer.

REFERENCES

[1] Institute for Traffic Accident Research and Data Analysis (ITARDA), "Statistics of Traffic Accident 2001", 2002. (in Japanese)
[2] Kahle W., Leonhardt H., Platzer W., "Tashenatlas der Anatomie", 1986
[3] Currey J. D., Butler G., "The Mechanical Properties of Bone Tissue in Children", JBJS [Am] 57A (6) 810-4, 1975.
[4] Shoenau E., Neu C. M., Rauch F., Manz F., "The Development of Bone Strength at the Proximal Radius during Childhood and Adolescence", Journal of Clinical Endocrinology and Metabolism, 86 (2) 613-8, 2001.
[5] Jones E., "Skeletal Growth and Development as Related to Trauma", In: Green N. E., Swiontkowski M. F., "Skeletal Trauma in Children", 2nd ed., Philadelphia, W B Saunders, 1998.
[6] Williams J. L., Do P. D., Eick J. D., Schmidt T. L., "Tensile properties of the physis vary with anatomic location, thickness, strain rate and age", Journal of Orthopaedic Research, 19 1043-8, 2001.
[7] Fujii T., Takai S., Arai Y., Kim W., Amiel D., Hirasawa Y., "Microstructural Properties of the Distal Growth Plate of the Rabbit Radius and Ulna: Biomechanical, Biochemical and Morphological Studies", Journal of Orthopaedic Research, 18 87-93, 2000.
[8] Ogden J. A., Ganey T. M., Ogden D. A., "The Biological Aspects of Children's Fractures", In: Rockwood C. A. Jr., Wilkins K. E., Beaty J. H., "Fractures in Children", Volume 3, 4th edition, Philadelphia, New York: Lippincott-Raven, p19-52, 1996.
[9] Amamilo S. C., Bader D. L., Houghton G. R., "The Periosteum in Growth Plate Failure", Clinical Orthopaedics and Related Research, 194 293-305, 1983.
[10] World Medical Association, "WORLD MEDICAL ASSOCIATION DECLARATION OF HELSINKI", http://www.wma.net, 1964.
[11] Araki C., Hara Y., "A key to pediatric imaging", Shujunsha Publishers P61-71, 2001. (in Japanese)
[12] Eveleth P. B., Tanner J. M., "Worldwide variation in human growth", Second edition, Cambridge University Press, 1990.
[13] Takahashi Y., Kikuchi Y., "Biofidelity of test devices and validity of injury criteria for evaluating knee injury to pedestrians", 17th International Technical Conference on the Enhanced Safety of Vehicles, 2001.